



HAL
open science

Calcium silicate hydrates investigated by solid-state high resolution 1H and 29Si nuclear magnetic resonance

Fabienne Meducin, B. Bresson, N. Lequeux, Marie-Noëlle de Noirfontaine, H. Zanni

► To cite this version:

Fabienne Meducin, B. Bresson, N. Lequeux, Marie-Noëlle de Noirfontaine, H. Zanni. Calcium silicate hydrates investigated by solid-state high resolution 1H and 29Si nuclear magnetic resonance. *Cement and Concrete Research*, 2007, 37, pp.631-638. 10.1016/j.cemconres.2007.01.011 . hal-00165017

HAL Id: hal-00165017

<https://hal.science/hal-00165017v1>

Submitted on 17 Mar 2021

HAL is a multi-disciplinary open access archive for the deposit and dissemination of scientific research documents, whether they are published or not. The documents may come from teaching and research institutions in France or abroad, or from public or private research centers.

L'archive ouverte pluridisciplinaire **HAL**, est destinée au dépôt et à la diffusion de documents scientifiques de niveau recherche, publiés ou non, émanant des établissements d'enseignement et de recherche français ou étrangers, des laboratoires publics ou privés.

Calcium silicate hydrates investigated by solid-state high resolution ^1H and ^{29}Si nuclear magnetic resonance

Fabienne Méducin ^{a,*}, Bruno Bresson ^b, Nicolas Lequeux ^c,
Marie-Noëlle de Noirfontaine ^d, Hélène Zanni ^a

^a *Laboratoire de Physique et Mécanique des Milieux Hétérogènes, Ecole Supérieure de Physique et Chimie Industrielles, 75231 Paris Cedex 05, France*

^b *Laboratoire de Physique Quantique, ESPCI, France*

^c *Laboratoire de Physico-Chimie des polymères et des milieux dispersés, ESPCI, France*

^d *Laboratoire CECM-CNRS, 15, rue Georges Urbain, 94407 Vitry sur Seine, France*

Received 1 September 2006; accepted 26 January 2007

Abstract

This work focuses on phases formed during cement hydration under high pressure and temperature: portlandite $\text{Ca}(\text{OH})_2$ (CH); hillebrandite $\text{Ca}_2(\text{SiO}_3)(\text{OH})_2$ (β -dicalcium silicate hydrate); calcium silicate hydrate (C–S–H); jaffeite $\text{Ca}_6(\text{Si}_2\text{O}_7)(\text{OH})_6$ (tricalcium silicate hydrate); α -C₂SH $\text{Ca}_2(\text{SiO}_3)(\text{OH})_2$ (α -dicalcium silicate hydrate); xonotlite $\text{Ca}_6(\text{Si}_6\text{O}_{17})(\text{OH})_2$ and kilchoanite $\text{Ca}_6(\text{SiO}_4)(\text{Si}_3\text{O}_{10})$. Portlandite and hillebrandite were synthesized and characterised by high resolution solid-state ^1H and ^{29}Si Nuclear Magnetic Resonance. In addition, information from the literature concerning the last five phases was gathered. In certain cases, a schematic 3D-structure could be determined. These data allow identification of the other phases present in a mixture. Their morphology was also observed by Scanning Electron Microscopy.

© 2007 Elsevier Ltd. All rights reserved.

Keywords: Hydration products; Temperature; Scanning Electron Microscopy; Spectroscopy; X-ray diffraction

1. Introduction

The study of cement hydration at high temperature and under high pressure (up to 200 °C and 1000 bar) is of great interest in forecasting the durability of oil well cements. During this process, a cement slurry is pumped into the steel casing of the well up the annular space between the casing and the surrounding rock to support and protect it. From the view point of oil and gas companies, the disappearance of the mechanical resistance of cement at high pressure and temperature is critical; it can lead to a loss of integrity of cemented annulus and, consequently, can stop production. It is therefore important to know the structure of the calcium silicate phases formed under such unusual conditions.

Cement hydration has been studied widely under conditions of normal temperature and pressure, and several studies have been carried out on model systems at higher temperatures [1–3]. The studies at high pressure concern mainly thermodynamic equilibrium between high temperature and high pressure phases in the ternary H_2O – CaO – SiO_2 system [4,5]. However, the results are not easily transposed to cement paste hydration since this system may not reach an equilibrium state (the hydrated phases formed are metastable) [6]. This paper focuses on the structure of calcium silicate hydrates which can be formed under high pressure and temperature: portlandite $\text{Ca}(\text{OH})_2$ (CH), hillebrandite $\text{Ca}_2(\text{SiO}_3)(\text{OH})_2$ (β -dicalcium silicate hydrate), calcium silicate hydrates (C–S–H), jaffeite $\text{Ca}_6(\text{Si}_2\text{O}_7)(\text{OH})_6$ (tricalcium silicate hydrate), α -C₂SH $\text{Ca}_2(\text{SiO}_3)(\text{OH})_2$ (α -dicalcium silicate hydrate), xonotlite $\text{Ca}_6(\text{Si}_6\text{O}_{17})(\text{OH})_2$, and kilchoanite $\text{Ca}_6(\text{SiO}_4)(\text{Si}_3\text{O}_{10})$. Subsequent text uses the notation of cement chemistry: C = CaO, S = SiO_2 , H = H_2O . The first two phases (portlandite CH and hillebrandite β -C₂SH) were synthesized and then characterised by high resolution ^1H

and ^{29}Si NMR. In addition, information contained in the literature concerning the last five phases was gathered, especially regarding crystallography which can be helpful to interpret the NMR spectra. In certain cases, a schematic 3D-structure could easily be determined. The results obtained allow the resolution of phase mixtures as was shown in three mixtures formed during Ca_3SiO_5 hydration under high pressure and temperature.

2. Experimental procedure

2.1. Synthesis

Portlandite $\text{Ca}(\text{OH})_2$ (CH) and hillebrandite $\text{Ca}_2(\text{SiO}_3)(\text{OH})_2$ (β -dicalcium silicate hydrate) were synthesized in the Laboratoire Céramiques et Matériaux Minéraux at the Ecole Supérieure de Physique et Chimie Industrielles de Paris.

2.1.1. Portlandite

Portlandite occurs both as a natural mineral and a synthetic product, obtained by the hydration of lime, CaO , under a nitrogen atmosphere to avoid formation of CaCO_3 , and then drying by acetone–ether.

2.1.2. Hillebrandite

Hillebrandite occurs as a natural mineral [7] but is difficult to prepare synthetically in a pure state. A mixture of CaO and quartz (grain size $10\ \mu\text{m}$), with a molar CaO/SiO_2 (C/S) ratio = 2 and a water/solid (W/S) ratio = 15, was heated at $200\ ^\circ\text{C}$ under steam pressure for 7 days, and then solvent dried by using acetone–ether.

2.1.3. C–S–H, jaffeite, $\alpha\text{-C}_2\text{SH}$, xonotlite and kilchoanite preparation

These five phases were not synthesized as pure products but can be formed (always in mixtures) during cement hydration under high pressure and temperature as follows. Synthetic tricalcium silicate C_3S (triclinic T1 structure) has been mixed at room temperature with a water/cement (W/C) ratio of 0.44, the standard consistency requirement of class G cement, used in oil well cementing [8]. The average grain size of C_3S determined by laser granulometry is $10.1\ \mu\text{m}$ and the specific surface reaches $3.15\ \text{g}/\text{cm}^3$. Free lime CaO ($\sim 1\%$) and C_2S ($\sim 0.5\%$) as impurities are respectively detected by X-ray diffraction and ^{29}Si NMR in the C_3S sample. The C_3S purity is therefore acceptable for hydration. Distilled water was used. In some cases, SiO_2 named “S8 Silica” (provided by B.J. Services) is added (W/C = 0.55) until the C/S ratio is 1.5. BET surface is $0.62\ \text{m}^2/\text{g}$ and half of the grains are smaller than $20.7\ \mu\text{m}$. S8 silica contains mainly crushed quartz but microcline KAlSi_3O_8 is present as impurity (which is not detected either by X-ray diffraction or by ^{29}Si NMR).

A Teflon pot filled up with this cement paste was placed in a high temperature and pressure cell described elsewhere [9]. Argon was used as the pressure transmitting gas. The pressure was regulated first, and then the external heating began once the pressure was constant. Stable pressure and temperature

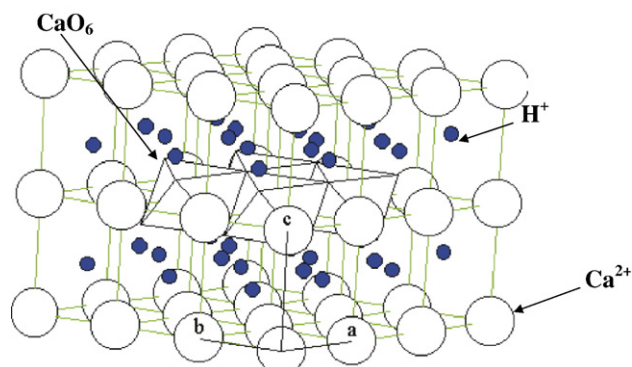
conditions were reached after half an hour, and the silicate sample was left in the cell to react. After a determined curing time, the pressure and temperature were rapidly dropped. After removal and crushing, the sample was analyzed.

2.2. Analyses

Hydrates were studied by a set of methods. First, the X-ray Diffraction (XRD) was performed on a Philips PW 1820 device, using $\text{Cu K}\alpha$ radiation, to characterize the crystal structures. Measurements were performed on powdered samples. The diffraction patterns were obtained in the range $2\theta = 10$ to 80° with a step of 0.03° and 4 s per step.

Both ^{29}Si and ^1H Nuclear Magnetic Resonance (NMR) were recorded to determine the characteristic peaks for each phase and to allow the quantification of mixtures [10]. The samples with ^{29}Si isotopic natural abundance (4.7%) were investigated using an ASX 300 Bruker spectrometer at a resonance frequency of 59.6 MHz. The pulse sequences used – MAS Single Pulse Experiment (SPE) and ^1H - ^{29}Si CPMAS (Cross-Polarized Magic Angle Spinning) – are well known in solid-state NMR [11,12]. The resolution is optimized with the signal of Q_8M_8 , $[\text{Si}(\text{CH}_3)_3]_8\text{Si}_8\text{O}_{20}$, which was used also as reference for the chemical shift measurement, giving a peak at 11.6 ppm. MAS Single Pulse and CPMAS experiments were performed with the following parameters: a $\pi/2$ pulse length of $3.3\ \mu\text{s}$, a spinning frequency of 5 kHz, a number of scans equal to 10,000, a recycle interval of 5 s and a contact time ranging from 1 to 10 ms in the CPMAS experiments. With the CPMAS experiments the dynamics of polarization of each phase are clearly seen to be in agreement with previous work [13,14].

^1H NMR experiments were performed on an ASX 300 Bruker spectrometer at a resonance frequency of 300 MHz on a sample with ^1H isotopic natural abundance ($\sim 100\%$). The pulse sequence used – CRAMPS (Combined Rotation And Multi Pulse Spectroscopy) [15] – is well known in solid-state ^1H -NMR [16,17]. It allows removal of the homonuclear proton–proton dipolar interaction, which broadens the peaks in MAS ^1H -NMR spectra. Resolution and calibration are adjusted with the signal of adamantane, $\text{C}_{10}\text{H}_{16}$, which gives a peak at 1.7 ppm. All the chemical shifts are given with ± 0.4 ppm accuracy.



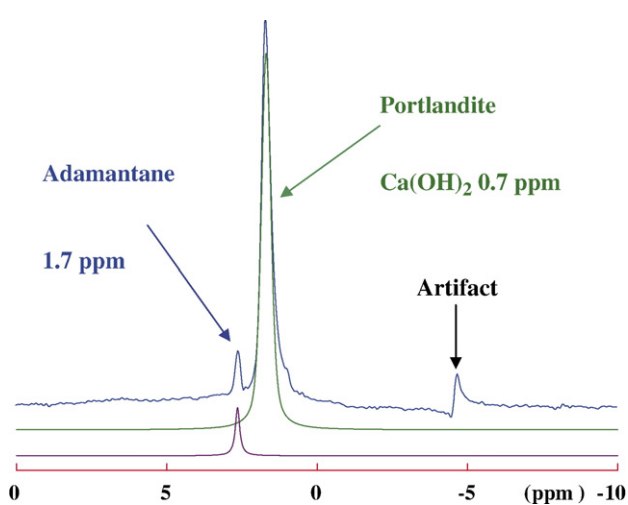


Fig. 2. $^1\text{H-NMR}$ CRAMPS spectrum of portlandite with adamantane.

Finally, Scanning Electron Microscopy (SEM) was used to observe the morphology of the different phases. Secondary electron images of fractures were performed on a JEOL 6300F field emission electron microscope. The samples were first coated with a thin metallic layer of platinum to increase the poor conductivity. The observations were recorded under a 4×10^{-6} Torr vacuum at 15 kV.

3. Results and discussion

3.1. Pure phases

3.1.1. Portlandite $\text{Ca}(\text{OH})_2$ (CH)

The unit cell of portlandite is hexagonal, with the following parameters $a=b=3.545 \text{ \AA}$ and $c=4.895 \text{ \AA}$, space group P-3m1 (trigonal) [18,19]. Hydrogen atom occupies only one crystallographic site ($1/3, 2/3, 0.437$). The positions for calcium and oxygen are respectively $(0,0,0)$ and $(1/3, 2/3, 0.233)$ [20,21]. Its performed diffraction pattern is in broad agreement with data in literature and is therefore not shown. In this phase, the CaO_6 octahedra share edge as can be seen in Fig. 1 (simulated structure by the software CaRIne).

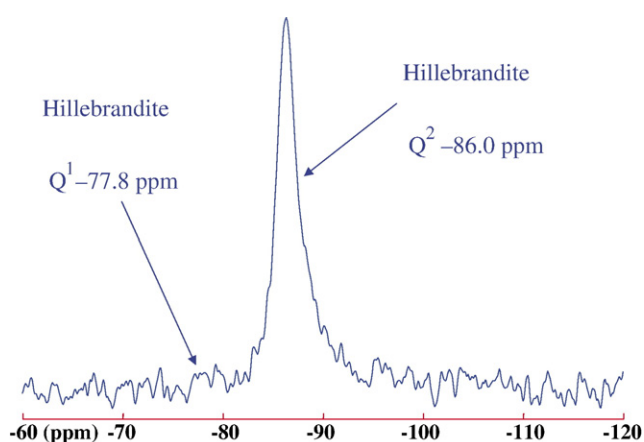


Fig. 3. $^{29}\text{Si-NMR}$ spectrum (SPE) of hillebrandite.

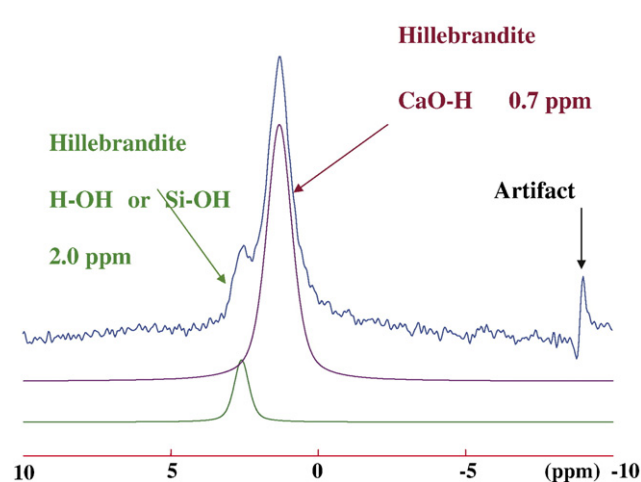


Fig. 4. $^1\text{H-NMR}$ CRAMPS spectrum of hillebrandite.

Moreover, this phase has been widely studied by $^1\text{H-NMR}$ [13,22]. Different pulse sequences (CRAMPS, MREV8) were used and a single peak (corresponding to the only crystallographic site) was found with an isotropic chemical shift equal to 0.7 ppm, which was obtained with the CRAMPS sequence in this study as well (Fig. 2). This peak corresponds to the hydrogen atom linked to the group Ca-O- , as specified in Heidemann's table of chemical shifts [22].

3.1.2. Hillebrandite, $\text{Ca}_2(\text{SiO}_3)(\text{OH})_2$ (β -dicalcium silicate hydrate)

This phase was synthesised according to the protocol given above and the analyses are then possible on the pure phase. The results obtained allow a comparison with literature values permitting the latter to be identified in phase mixtures.

The unit cell of the structure is orthorhombic with $a=3.6389 \text{ \AA}$, $b=16.311 \text{ \AA}$ and $c=11.829 \text{ \AA}$; Cmc21 [23,24]. The hydrogen atom can be found in two fully occupied crystallographic sites; silicon has two crystallographic sites as well but the occupancy is half for both [24]. The purity of the phase is checked by XRD and hillebrandite is the only phase

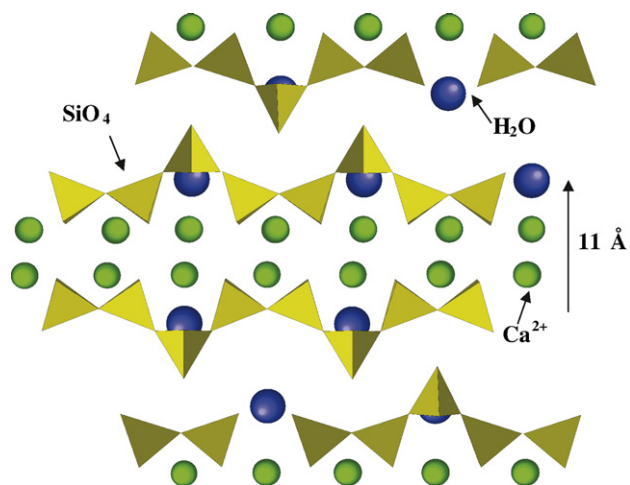


Fig. 5. Structure of C-S-H [20], courtesy of J.Minet.

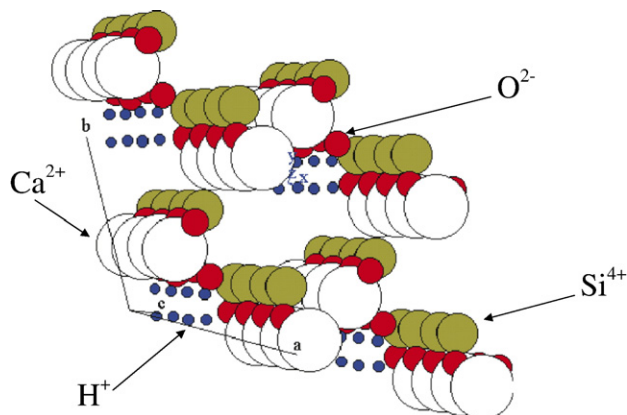


Fig. 6. Crystal structure of jaffeite.

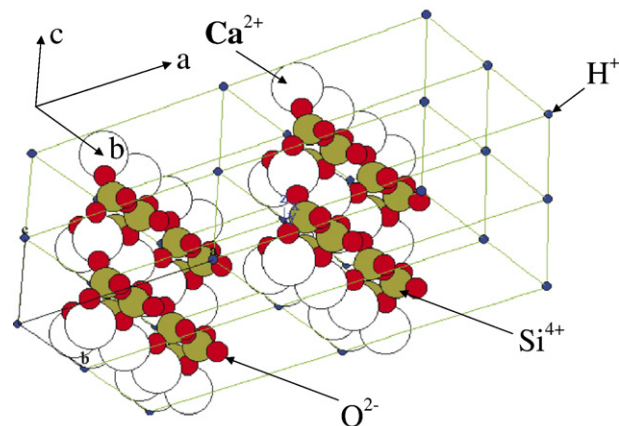


Fig. 8. Crystal structure of xonotlite.

detected. The diffraction pattern performed brings no new scientific insights and is therefore not presented.

The recorded ^{29}Si -NMR spectrum (MAS SPE) is provided in Fig. 3. Two peaks are observed at -86.0 ppm (corresponding to Q^2 entities) and -77.8 ppm (corresponding to Q^1 entities, undetectable on the SPE but clearly observed on the CPMAS spectrum) in agreement with Michel and Engelhardt's table of chemical shifts where Q^n stands for a SiO_4 tetrahedron linked to n other tetrahedra [25]. This result is consistent with previous reports [26,27].

In the ^1H -NMR spectrum obtained with the CRAMPS sequence, two peaks are found at 2.0 and 0.7 ppm (Fig. 4). The first peak is related to the H atom connected with $\text{Si}-\text{O}-$ (or with $\text{H}-\text{O}-$) and the second to the H atom connected to $\text{Ca}-\text{O}-$ in hillebrandite (no portlandite detected by XRD). Therefore, the two different crystallographic sites cannot be distinguished by CRAMPS. The spectrum given has been performed without the adamantane – added later as a reference – to confirm the chemical shifts.

3.1.3. Crystallographic data concerning the other phases

The five other phases were not synthesised but crystallographic data from the literature provide useful information in understanding NMR spectra and in the identification of different phases in a mixture.

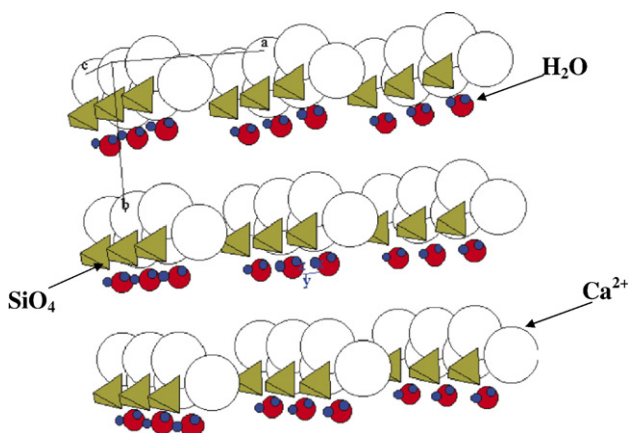
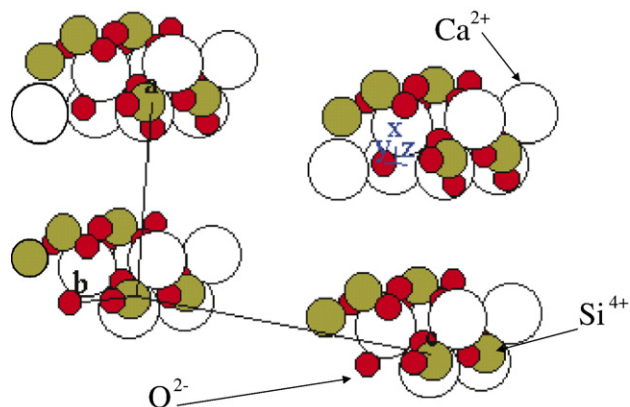


Fig. 7. Crystal structure of α -dicalcium silicate hydrate.

3.1.3.1. Calcium silicate hydrates (C-S-H). C-S-H are poorly crystallized and non-stoichiometric [6,28]. A structure has nevertheless been reported at room temperature [28]. Fig. 5 shows the double Ca-layers and the SiO_4 tetrahedrons chains (Q^1 and Q^2 entities). Isotropic chemical shifts between -70 and -92 ppm for the ^{29}Si -NMR are then expected for this phase in a mixture, in agreement with Michel and Engelhardt's table of chemical shifts [25].

3.1.3.2. Jaffeite $\text{Ca}_6(\text{Si}_2\text{O}_7)(\text{OH})_6$ (tricalcium silicate hydrate). Tricalcium silicate hydrate has been found as a natural mineral and could be prepared synthetically by hydrothermal treatment at 200 °C to 450 °C of Ca_3SiO_5 or other suitable starting material of similar C/S ratio, according to the literature [26]. Its space group is P3 (hexagonal lattice: $a=b=10.035$ Å and $c=7.499$ Å) [29]. The structure is shown in Fig. 6. Calcium planes and SiO_4 long chains (Q^2 entities) are clearly observed.

3.1.3.3. α - C_2SH $\text{Ca}_2(\text{SiO}_3)(\text{OH})_2$ (α -dicalcium silicate hydrate). The space group of α -dicalcium silicate hydrate is $\text{P}2_12_12_1$ with an orthorhombic lattice and the following parameters: $a=9.476$ Å, $b=9.198$ Å and $c=10.648$ Å. The hydrogen atom fully occupies crystallographic sites at (0.238,



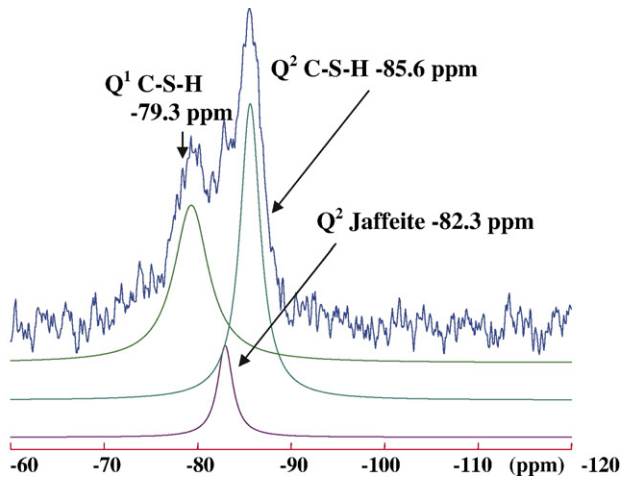


Fig. 10. ^{29}Si -NMR spectrum (SPE) of the C_3S hydrated sample at 120°C under 400 bar for 4 days.

0.438, 0.110) and (0.406, 0.413, 0.339) [30]. The simulated structure (Fig. 7) shows calcium layers and isolated SiO_4 tetrahedrons (Q^0 entities).

3.1.3.4. *Xonotlite* $\text{Ca}_6(\text{Si}_6\text{O}_{17})(\text{OH})_2$. Xonotlite in monoclinic $\text{P}2_1/a$, with $a=17.032\text{ \AA}$, $b=7.363\text{ \AA}$ and $c=7.012\text{ \AA}$; $\beta=90.36^\circ$ [31]. The simulated structure shows successive calcium and SiO_4 tetrahedrons layers (Fig. 8). The Q^2 entities are clearly identified here. We are then able to predict isotropic chemical shifts for the ^{29}Si -NMR between -75 and -92 ppm if this phase is part of a mixture [25].

3.1.3.5. *Kilchoanite* $\text{Ca}_6(\text{SiO}_4)(\text{Si}_3\text{O}_{10})$. Kilchoanite occurs in nature and also as a synthetic. Previous work shows $a=11.433\text{ \AA}$, $b=5.08\text{ \AA}$ and $c=22.017\text{ \AA}$, orthorhombic $\text{Im}a2$ [32]. The simulated structure (by CaRIne) shows calcium and SiO_4 tetrahedrons layers (Fig. 9) where Q^0 entities and Q^2 entities could be identified.

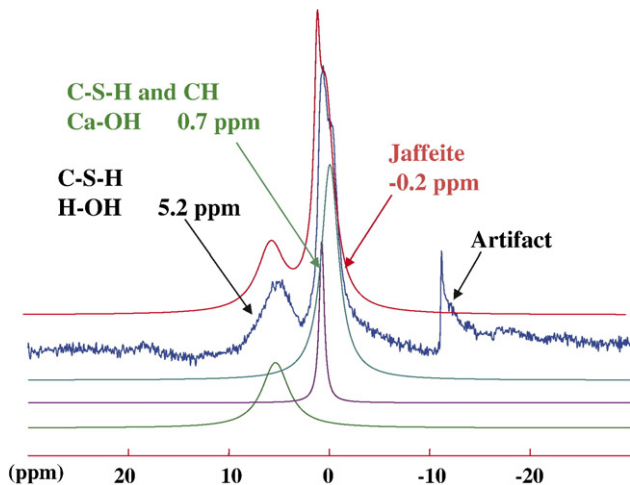


Fig. 11. ^1H -NMR CRAMPS spectrum of the C_3S hydrated sample at 120°C under 400 bar for 4 days.

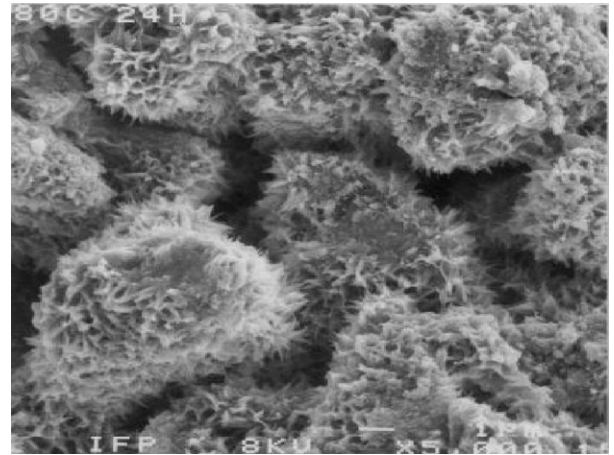


Fig. 12. SEM image of secondary electrons ($\times 5000$) of the C-S-H.

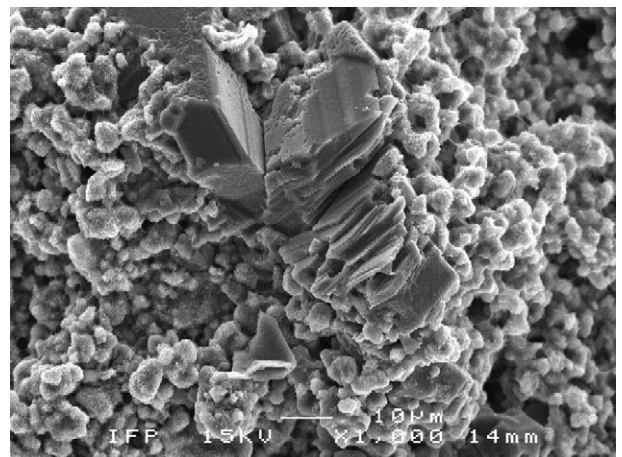
3.2. Identification of phases in mixtures

During oil well cementing, the hydration of C_3S may take place under high pressure and temperature and a mixture of calcium silicate hydrates is formed. Through the identification of the two first phases, portlandite and hillebrandite, by ^{29}Si -NMR and ^1H -NMR CRAMPS and the crystallographic data gathered from the literature, the other phases can be identified with the following method. Three samples were investigated, they were formed respectively at 120°C , 400 bar for 4 days; 200°C , 600 bar for 14 days and 200°C , 600 bar for 4 days with silica addition.

3.2.1. C_3S hydration at 120°C 400 bar for 4 days

X-Ray powder diffraction identifies as crystalline phases (jaffeite $\text{Ca}_6(\text{Si}_2\text{O}_7)(\text{OH})_6$, portlandite $\text{Ca}(\text{OH})_2$ and calcite CaCO_3).

Fig. 10 shows the ^{29}Si -NMR SPE MAS spectrum for a C_3S sample hydrated at 120°C , under 400 bar for 4 days. Three peaks are observed at -85.6 and -82.3 ppm (corresponding to Q^2 entities, i.e. SiO_4 tetrahedra in the middle of silicate chains) and -79.3 ppm corresponds to Q^1 entities, tetrahedra at the ends of silicate chains [25]. The peaks at -85.6 and -79.3 are very broad showing that the observed phase is poorly crystallized. Its



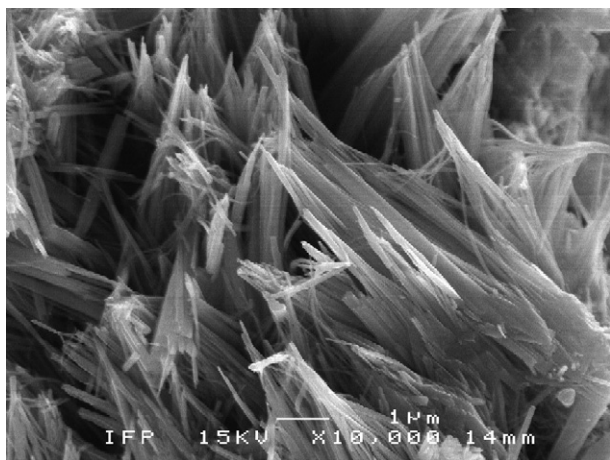


Fig. 14. SEM image of secondary electrons ($\times 10,000$) of jaffeite.

full width at half maximum height is ~ 4 ppm. The third peak, at -82.3 ppm, is not so broad and CPMAS experiments (given elsewhere [10]) at different contact times, 1, 5 and 10 ms, were undertaken to highlight the presence of two different phases. Previous work shows that the peak at -82.3 ppm is due to jaffeite [13] and this is in agreement with its crystal structure in which Q^2 entities were clearly identified (Fig. 6). Fig. 11 shows the $^1\text{H-NMR}$ CRAMPS spectrum of this sample. Two peaks are detected at around 4.8 ppm (H linked to $-\text{OSi}$ or $-\text{OH}$), 0.7 ppm and a shoulder at -0.2 ppm (H linked to $-\text{OCa}$). It confirms the presence of portlandite in the sample (also detected by X-ray diffraction) from the chemical shift at 0.7 ppm. The presence of C-S-H in the sample is highlighted through peaks at around 4.8 ppm and 0.7 ppm, as reported in the literature [13,17]. The peak at 0.7 ppm (H linked to $-\text{OCa}$) is a contribution from CH and C-S-H . The only peak not yet attributed must be the CRAMPS signature of jaffeite, detected in the mixture by XRD and $^{29}\text{Si-NMR}$: the chemical shift for jaffeite is then -0.2 ppm.

This sample has been investigated by SEM and the following morphologies have been determined. Fig. 12 gives a C-S-H morphology, which forms radiating clusters with numerous disordered needles [6,33]. Fig. 13 shows blocks of

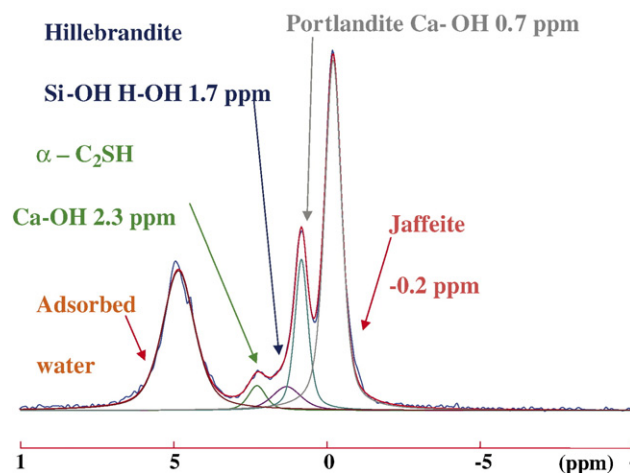


Fig. 16. $^1\text{H-NMR}$ CRAMPS spectrum of the C_3S hydrated sample at 200°C under 600 bar for 14 days.

portlandite, the composition of which was determined by dispersive X-ray analysis. This analysis clearly confirms that there was no silicon in these blocks, only calcium and oxygen (hydrogen was not detected). The only phase containing no silicon in the sample is CH. The morphology of jaffeite is said to be acicular [33] and the only other morphology found in the considered sample were the organized needles (fasciae), as shown in Fig. 14.

3.2.2. C_3S hydration at 200°C 600 bar for 14 days

The phases formed during the hydration of a C_3S sample at 200°C under 600 bar for 14 days were examined. XRD detects portlandite, hillebrandite, jaffeite and α -dicalcium silicate hydrate. Fig. 15 gives the $^{29}\text{Si-NMR}$ MAS spectrum for this sample. Three peaks are observed at -86.0 ppm (hillebrandite); -82.3 ppm (jaffeite) and -72.4 ppm. The latter corresponds to Q^0 entities in α -dicalcium silicate hydrate. This assignment agrees with the structure of $\alpha\text{-C}_2\text{SH}$ (Fig. 7).

The same sample, investigated by $^1\text{H-NMR}$ CRAMPS (Fig. 16), gives four peaks: at 2.3 ppm, 1.7 ppm (hillebrandite), 0.7 ppm (portlandite) and -0.2 ppm (jaffeite). A fifth peak for adsorbed water can be seen at around 5 ppm. The peak at

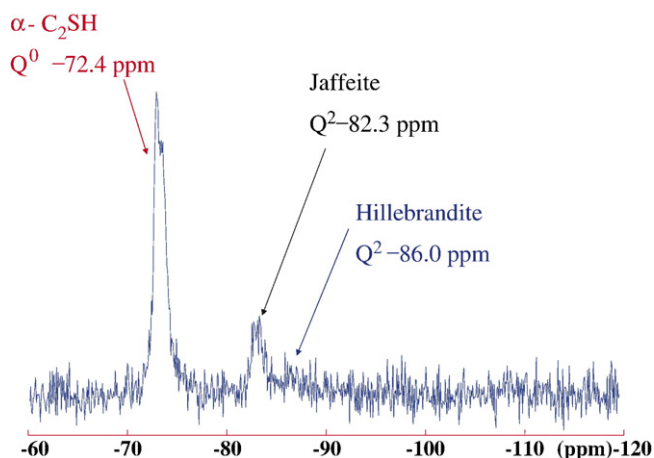
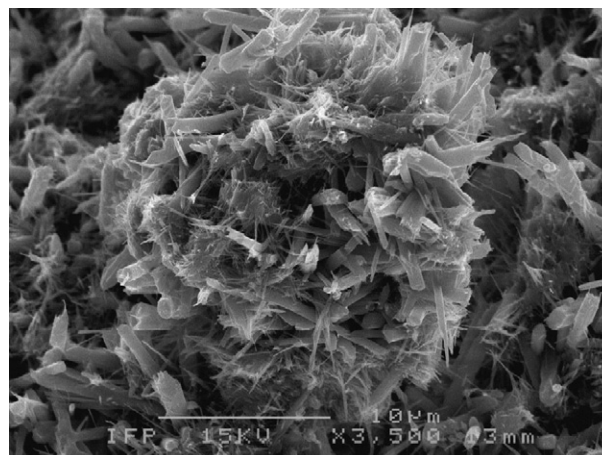


Fig. 15. $^{29}\text{Si-NMR}$ spectrum (SPE) of the C_3S hydrated sample at 200°C under 600 bar for 14 days.



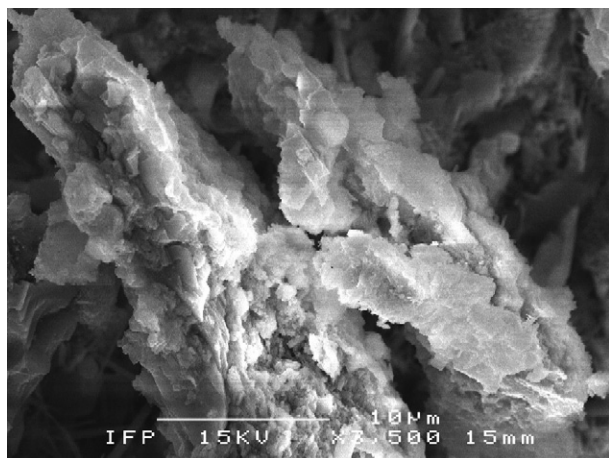


Fig. 18. SEM image of secondary electrons ($\times 3500$) of α -dicalcium silicate hydrate.

2.3 ppm is consequently the signature of α -dicalcium silicate hydrate. In the literature, this phase is said to give two $^1\text{H-NMR}$ CRAMPS peaks at 2.3 ppm and -9.6 ppm [17,22], but our work only shows clearly the former.

Previous work shows that hillebrandite has an acicular disordered morphology [33] and such needles are indeed found in the present sample (Fig. 17). The morphology of α -dicalcium silicate hydrate is said to be acicular [33] but is not often observed owing to the damage by the microprobe electron beam [6]. However, a cloudy aspect could be seen for the studied sample, which corresponds to none of the other morphologies found in Fig. 18.

3.2.3. C_3S hydration at 200 °C 600 bar for 4 days with silica addition

The phases formed after the hydration of tricalcium silicate under 200 °C and 600 bar for 4 days with silica addition ($\text{W/C}=0.55$; $\text{C/S}=1.5$) have been investigated. The phases detected by XRD are kilchoanite, xonotlite and α -dicalcium silicate

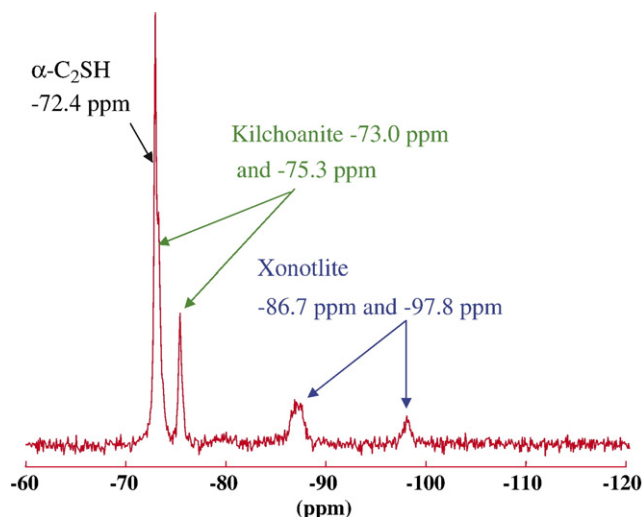


Fig. 19. $^{29}\text{Si-NMR}$ spectrum (SPE) of the C_3S hydrated sample at 200 °C under 600 bar for 4 days with silica addition.

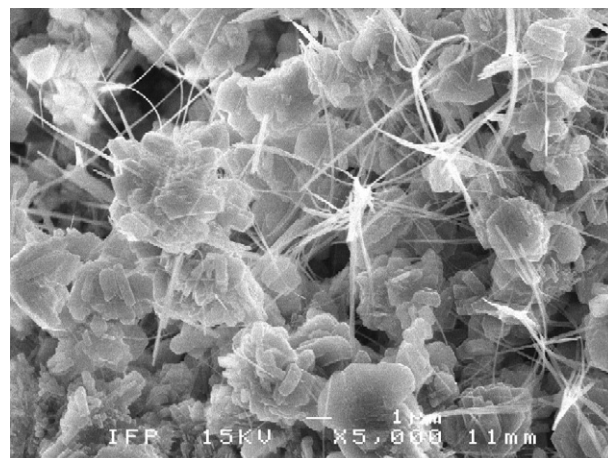


Fig. 20. SEM image of secondary electrons ($\times 5000$) of xonotlite (fibres) and kilchoanite (globules).

hydrate. The added silica was not detected and should have totally reacted.

The $^{29}\text{Si-NMR}$ spectrum of the sample is given Fig. 19. Five peaks are observed, at -72.4 ppm (α -dicalcium silicate hydrate) with a shoulder around -73.0 ppm, -75.3 ppm, -86.7 ppm (broad peak) and -97.8 ppm. The four latter peaks can be assigned to xonotlite and kilchoanite with the help of literature data. Spectra of xonotlite are found for single pulse (MAS) and cross-polarization experiments (CPMAS with a 3 ms contact time) in the literature [26]. Three peaks are observed for this phase at -86.7 and -97.7 ppm (corresponding to Q^2 and Q^3 entities respectively) and -79.8 ppm corresponding to Q^1 entities, undetectable on the single pulse spectrum. Consequently, the peaks at -86.7 ppm and -97.8 ppm observed in our work can be attributed to xonotlite, although the peak expected at -79.8 ppm was not clearly detected. The $^{29}\text{Si-NMR}$ MAS spectra of kilchoanite found in the literature are for single pulse (MAS) and cross-polarization experiments (CPMAS with a 3 ms contact time) [26]. Three peaks are observed at -73.1 and -75.3 ppm (corresponding to Q^0 entities identified

on Fig. 13) and Q^2 entities at -85.6 ppm. Bell et al. synthesized this phase at low temperature which explains the presence of water on its surface and the possibility of observing a CPMAS spectrum [26]. In our work, the signatures of the kilchoanite are the following: the most intense peak of the literature (at -73.1 ppm) is certainly the shoulder detected at -73.0 ppm and the peak at -75.3 ppm is readily detected, in agreement with Bell's work. The third peak of the literature may not be differentiated from the broad peak we found at -86.7 ppm.

The ^1H -NMR CRAMPS spectrum of the sample is not given since the xonotlite position could not be clearly identified. The position for the α -dicalcium silicate hydrate peak is known from the previous sample studied (2.3 ppm). The amount of xonotlite in the sample is probably not sufficient to identify clearly its peak. Alternatively both phases could give coincident peaks. Only the synthesis of pure xonotlite would resolve this point.

This sample was observed by SEM, previous work shows that xonotlite has an acicular morphology [33]. Fig. 20 shows xonotlite fibres connected to kilchoanite globules (the most abundant phase identified through the others analysis methods excluding α -dicalcium silicate hydrate).

4. Conclusion

Table 1 gives the characterization of each phase reviewed in this paper. The morphology is obtained by SEM images of secondary electrons and confirms data from the literature. The isotropic chemical shifts for ^{29}Si -NMR as well as for ^1H -NMR are given with an accuracy of ± 0.4 ppm.

Acknowledgements

The authors are grateful to Pierre Tougne and Victor Moulancier for expert technical support during CRAMPS experiments. FM kindly acknowledges Dr Sharon Ashbrook and Dr Karl Whittle for helpful discussions and suggestions.

References

- [1] E.R. Buckle, H.F.W. Taylor, The hydration of tricalcium and dicalcium silicates in pastes under normal and steam curing conditions, *J. Appl. Chem.* 9 (1959) 163–172.
- [2] I. Odler, Hydration of tricalcium silicate at elevated temperature, *J. Appl. Chem. Biotechnol.* 23 (1973) 661–667.
- [3] S. Masse, H. Zanni, J. Lecourtier, J.C. Roussel, A. Rivereau, High temperature hydration of tricalcium silicate, the major component of portland cement: a ^{29}Si NMR Contribution, *J. Chem. Phys.* 92 (1995) 1861–1866.
- [4] I. Harker, Dehydration series in the system $\text{CaSiO}_3\text{--SiO}_2\text{--H}_2\text{O}$, *J. Am. Ceram. Soc.* 47 (1964) 521–529.
- [5] C.W.F.T. Pistorius, Thermal decomposition of portlandite and xonotlite to high pressures and high temperatures, *Am. J. Sci.* 261 (1963) 79–83.
- [6] H.W.F. Taylor, *Cement Chemistry*, 2nd edition, Thomas Telford Edition, London, 1997.
- [7] F.E. Wright, On three contact minerals from Velardena, Durango, Mexico (gehlenite, spurrite and hillebrandite), *Am. J. Sci.* 4 (26) (1908) 545–554.
- [8] C. Noik, A. Rivereau, Oilwell cement durability, SPE annual technical conference and exhibition, Houston, Texas, 3–6 October, 1996.
- [9] F. Méducin, B. Bresson, H. Zanni, C. Noik, G. Hamel, Effect of high pressure on tricalcium silicate hydration at normal temperature and at 200 °C, *Cem. Concr. Res.*, submitted for publication.
- [10] F. Méducin, C. Noik, A. Rivereau, H. Zanni, Complementary analyses of a tricalcium silicate hydrated at high pressure and temperature, *Cem. Concr. Res.* 32 (2002) 65–70.
- [11] E. Lippmaa, M. Mägi, M. Tarmak, W. Wiekler, A.R. Grimmer, A high resolution ^{29}Si NMR study of the hydration of tricalcium silicate, *Cem. Concr. Res.* 12 (1982) 597–602.
- [12] S.A. Rodger, G.W. Groves, N.J. Clayden, C.M. Dobson, Hydration of tricalcium silicate followed by ^{29}Si NMR with cross-polarization, *J. Am. Ceram. Soc.* 71 (2) (1988) 91–96.
- [13] B. Bresson, H. Zanni, Pressure and temperature influence on tricalcium silicate hydration. A ^1H and a ^{29}Si NMR study, *J. Chem. Phys.* 95 (1998) 327–331.
- [14] B. Bresson, S. Masse, H. Zanni, C. Noik, Tricalcium silicate hydration at high temperature. A ^{29}Si and a ^1H investigation, in: P. Colombet, A.-R. Grimmer, H. Zanni, P. Sozzani (Eds.), *Nuclear Magnetic Resonance Spectroscopy of Cement-Based Materials*, Springer-Verlag, Berlin, 1998, pp. 333–343.
- [15] B.C. Gerstein, CRAMPS, in: D.M. Grant, R.K. Harris (Eds.), *Encyclopedia of Nuclear Magnetic Resonance*, vol. 3, Wiley, 1996, pp. 1501–1509.
- [16] B. Bresson, H. Zanni, S. Masse, C. Noik, Contribution of ^1H combined rotation and multipulse spectroscopy nuclear magnetic resonance to the study of tricalcium silicate hydration, *J. Mater. Sci.* 32 (1997) 4633–4639.
- [17] D. Heidemann, W. Wiekler, Characterization of protons in C–S–H phases by means of high-speed ^1H MAS NMR investigation, in: P. Colombet, A.-R. Grimmer, H. Zanni, P. Sozzani (Eds.), *Nuclear Magnetic Resonance Spectroscopy of Cement-Based Materials*, Springer-Verlag, Berlin, 1998, pp. 169–180.
- [18] H.D. Megaw, The thermal expansions of certain crystals with layer lattices, *Proc. Roy. Soc. A* 142 (846) (1933) 198–214.
- [19] D.M. Henderson, H.S. Gutowski, A nuclear magnetic resonance determination of the hydrogen positions in $\text{Ca}(\text{OH})_2$ at $T=25$ °C, *Am. Mineral.* 47 (1962) 1231–1251.
- [20] A. Winchell, H. Winchell, *Microscopic Character of Artificial Inorg. Solid Sub*, 1964.
- [21] H.E. Petch, The hydrogen positions in portlandite, $\text{Ca}(\text{OH})_2$, as indicated by the electron distribution, *Acta Crystallogr.* 14 (1961) 950–957.
- [22] D. Heidemann, Proton high-resolution solid-state NMR spectroscopy using CRAMPS techniques for studies in silicate and cement science, in: P. Colombet, A.R. Grimmer (Eds.), *Application of NMR Spectroscopy to Cement Science*, Guerville, 1992, Gordon and Breach, Paris, 1994, pp. 77–102.
- [23] L. Heller, X-Ray investigation of hillebrandite, *Mineral. Mag.* 30 (1953) 150–154.
- [24] Y. Dai, J.E. Post, Crystal structure of hillebrandite: a natural analogue of calcium silicate hydrate (CSH) phases in Portland cement, *Am. Mineral.* 80 (1995) 841–844.
- [25] G. Engelhardt, D. Michel, *High-Resolution Solid-State NMR of Silicates and Zeolites*, Wiley, New York, 1989.
- [26] G.M.M. Bell, J. Bensted, F.P. Glasser, E.E. Lachowski, D.R. Roberts, M.J. Taylor, Study of calcium silicate hydrates by solid state high resolution ^{29}Si nuclear magnetic resonance, *Adv. Cem. Res.* 3 (9) (1990) 23–37.
- [27] X. Cong, R.J. Kirkpatrick, ^{29}Si and ^{17}O NMR investigation of the structure of some crystalline calcium silicate hydrates, *Adv. Cem. Based Mater.* 3 (1996) 133–143.
- [28] I. Klur, B. Pollet, J. Virlet, A. Nonat, C–S–H structure evolution with calcium content by multinuclear NMR, in: P. Colombet, A.-R. Grimmer, H. Zanni, P. Sozzani (Eds.), *Nuclear Magnetic Resonance Spectroscopy of Cement-Based Materials*, Springer-Verlag, Berlin, 1998, pp. 119–141.
- [29] N.A. Yamnova, C.H. Sarp, Y.K. Egorov-Tismensko, D.Y. Pucarovsky, Crystal structure of jaffeite, *Krystallografiya* 38 (4) (1993) 73–78.
- [30] R.E. Marsh, A revised structure for α -dicalcium silicate hydrate, *Acta Crystallogr. C50* (1994) 996–997.
- [31] C. Hejny, Th. Armbruster, Polytypism in xonotlite $\text{Ca}_6\text{Si}_6\text{O}_{17}(\text{OH})_2$, *Z. Kristallogr.* 216 (7) (2001) 396–408.
- [32] M. Kimata, The crystal structure of manganian kilchoanite, $\text{Ca}_{2.33}\text{Mn}_{0.67}\text{Si}_2\text{O}_7$: a site-preference rule for the substitution of Mn for Ca, *Mineral. Mag.* 53 (1989) 625–631.
- [33] E. Schlegel, R. Strienitz, Faserförmige Kalziumsilikathydrate, *Silikattechnik* 41 (8) (1990) 278–283.